NANO LETTERS

Letter

pubs.acs.org/NanoLett

DNA-Controlled Excitonic Switches

Elton Graugnard,*[,†] Donald L. Kellis,[‡] Hieu Bui,[§] Stephanie Barnes,[†] Wan Kuang,[§] Jeunghoon Lee,[∥] William L. Hughes,[†] William B. Knowlton,[†,§] and Bernard Yurke[†,§]

[†]Department of Materials Science and Engineering, [‡]Department of Biological Sciences, [§]Department of Electrical and Computer Engineering, [∥]Department of Chemistry and Biochemistry, Boise State University, Boise, Idaho 83725, United States

Supporting Information

ABSTRACT: Fluorescence resonance energy transfer (FRET) is a promising means of enabling information processing in nanoscale devices, but dynamic control over exciton pathways is required. Here, we demonstrate the operation of two complementary switches consisting of diffusive FRET transmission lines in which exciton flow is controlled by DNA. Repeatable switching is accomplished by the removal or addition of fluorophores through toehold-mediated strand invasion. In principle, these switches can be networked to implement any Boolean function.

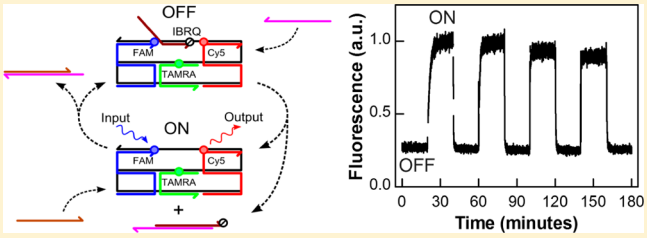

KEYWORDS: *DNA, FRET, excitonic switch, molecular transmission line, molecular programming, Boolean logic*

One of the driving forces in the field of nanotechnology is the development of highly compact information processing devices. A potential method for nanoscale circuit construction is the use of individual molecules as circuit elements with an emphasis on bottom-up fabrication techniques and self-assembly.[1] Molecular photonic devices show promise as a means for information processing at the nanoscale.[2,3] Diffusive energy transfer in molecular photonic devices may be achieved between neighboring molecules through fluorescence resonance energy transfer (FRET), which involves the direct transfer of excitonic energy between fluorophores via the dipole−dipole coupling.[4]

One challenge associated with the implementation of FRET in devices is the precise nanometer scale positioning of fluorophores into arrangements that promote efficient energy transfer. DNA nanotechnology provides a well-defined, programmable framework for manipulating fluorophores at the molecular level.[1,5−15] Multiple studies have reported spectroscopic techniques for obtaining information concerning the structure and photonic properties of fluorophores bound to DNA molecules.[16−19] For instance, FRET has been used as a means for measuring distances in DNA and RNA helices by binding donor and acceptor fluorophores to specific nucleotides and extrapolating their separation distance from the measured FRET efficiency.[16,19] DNA origami techniques have been used to arrange fluorophores as well, introducing greater structural rigidity and design flexibility to DNA-based FRET devices.[14,15]

The ability to dynamically control FRET is essential if it is to be used effectively in circuit design. Hannestad et al. recently reported a FRET-based photonic network in which the excitation energy can be directed to either of two outputs based on the presence of an intercalating dye.[20] Here, we report two DNA-controlled FRET-based switches that were devised to enable programmable dynamic control of excitonic energy flow. The strand invasion process[21] that turns one switch off through the removal of a fluorophore turns the other switch on through the removal of a quencher. A second strand invasion process restores the chromophores, allowing the switches to be repeatedly cycled through their on and off states. The two switches are complementary in that one accomplishes the logical negation of the function carried out by the other switch. Logical AND functionality can be implemented by cascading such switches in series, and logical OR functionality can be implemented by combining such switches in parallel. In principle, such switches can be networked to implement any Boolean function where the absence or presence of excitonic energy transfer through a switch corresponds to a logical zero or one, respectively, and the output is the absence or presence of a fluorescence signal on the output fluorophore.

To explore the viability of switching in molecular scale photonic circuits, two distinct approaches were employed to enable dynamic control over the switch emission state. The designs, labeled Switch 1 and Switch 2, are illustrated in Figure 1 panels a and b, respectively, and the strand sequences and dye details are provided in the Supporting Information S1. Both switches consist of a serpentine DNA scaffold strand (black) hybridized with three staple strands using eight independent sequence domains, each 14 nucleotides (nt) long, that are separated by crossovers. A fourth "control" strand regulates excitonic energy flow within the switch, as discussed below. One of the staple strands (blue) contains the input dye FAM. Another staple strand (red) contains the output dye Cy5. In

Received: February 2, 2012
Revised: February 27, 2012
Published: March 8, 2012

   dx.doi.org/10.1021/nl3004336 | *Nano Lett.* 2012, 12, 2117−2122

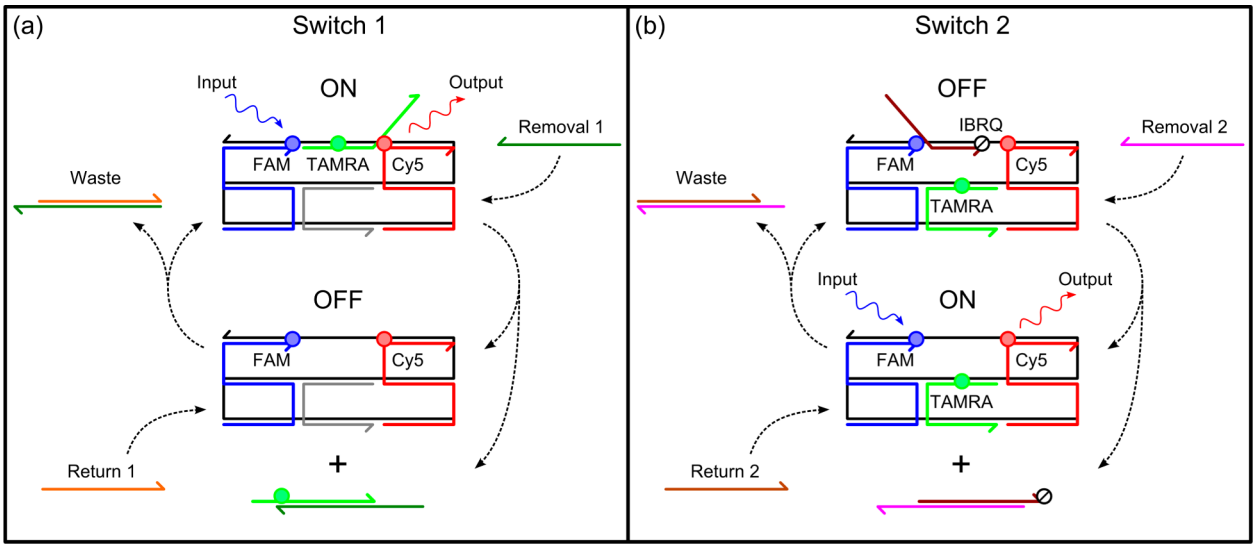

Figure 1. Schematic of the cyclic process for switching the dynamic FRET-based transmission lines by DNA strand invasion. (a) When Switch 1 is in its ON state, the TAMRA-functionalized control strand (green) is attached to the scaffold (black), resulting in an intact transmission line. The Removal 1 strand (dark green) hybridizes with the control strand, removing the TAMRA dye from the scaffold and interrupting FRET, which switches the device to its OFF state. To restore FRET and return the device to its ON state, the Return 1 strand (orange) hybridizes with the Removal 1 strand, releasing the control strand and allowing the TAMRA dye to rejoin with the scaffold. (b) When Switch 2 is in its OFF state, the IBRQ(quencher)-functionalized control strand (brown) is attached to the scaffold, quenching Cy5 emission. When the control strand is displaced by the Removal 2 strand (pink), emission is no longer suppressed and the device enters its ON state. When the control strand is restored via the Return 2 strand (dark orange), emission is once again suppressed, returning the device to its OFF state. The lengths of all strands and toeholds are drawn approximately to scale.

Switch 1 (Figure 1a), the third staple strand (gray) provides structural integrity, while the control strand (green) contains the intermediate dye TAMRA. When all five strands are hybridized, Switch 1 is in the ON state, and seven base pairs (bp) separate the input dye from the intermediate dye and the intermediate dye from the output dye. The three dyes of Switch 1 form a linear excitonic transmission line along a single DNA double-helix allowing excitation energy to flow from the input dye through the intermediate dye to the output dye.

To dynamically regulate energy flow, the control strand possesses a 14 nt long toehold sequence that allows it to be removed from the switch by toehold-mediated strand invasion.[21] For Switch 1, the removal strand (Removal 1 in Figure 1a) is complementary to the toehold of the control strand and to 10 of the 14 nucleotides binding the control strand to the switch. When the removal strand fully hybridizes with the control strand, only four nucleotides bind the control strand to the switch scaffold, and the control strand spontaneously dissociates from the scaffold.[22] As illustrated in Figure 1a, with TAMRA removed, FRET-based energy transmission is possible only by direct transfer between FAM and Cy5. On the basis of the ~5 nm separation and low spectral overlap, the coupling efficiency for direct FAM to Cy5 transfer is low, and Switch 1 is in its OFF state. In order to restore the switch to its ON state, the removal strand contains a 10 nt long toehold allowing it to be separated from the control strand by a second strand invasion, producing an unreactive waste product. The return strand (Return 1 in Figure 1a) is complementary to all but five of the removal strand nucleotides. Although this design requires the control strand to spontaneously dissociate from the removal strand, it minimizes the sequence commonality of the control and return strands to only five nucleotides. Thus, direct interaction of the return strand with the scaffold of the switch should be minimal. Once the control strand is displaced from the removal strand, the control strand can rehybridize with the switch scaffold and restore Switch 1 to its ON state.

Switch 2 (Figure 1b) is slightly more complex than Switch 1 and was designed to exhibit the complementary (inverse) behavior. In Switch 2, the third staple strand (green) contains the intermediate TAMRA dye, while the control strand (brown) contains an Iowa Black Red Quencher (IBRQ) at its 3′ end. The IBRQ is positioned within two nucleotides of the output Cy5. Thus, when all five strands are hybridized, Switch 2 is in the OFF state; energy flow from FAM to TAMRA to Cy5 is allowed, but emission from Cy5 is suppressed by energy transfer to IBRQ. Similar to Switch 1, the control strand can be removed by strand invasion with a removal strand (Removal 2 in Figure 1b). With the IBRQ removed from the switch, Switch 2 is in its ON state: excitonic energy can flow from FAM through TAMRA to Cy5, and Cy5 emission is allowed. Restoration of Switch 2 to the OFF state is achieved by strand invasion with a return strand (Return 2 in Figure 1b), similar to Switch 1. On the basis of these complementary switch designs, logical high transitions in one switch correspond to logical low transitions in the other.

All oligonucleotides for the switches were purchased lyophilized from Integrated DNA Technologies, rehydrated in filtered ultrapure water (Milli-Q Water, Millipore), and used without further purification (sequences and manufacturer purification methods are listed in Supporting Information S1). The switches were synthesized through self-assembly by combining the scaffold strand with the 20% molar excess of the staple strands in a solution of 1×TAE, Mg^{2+} (40 mM tris, 20 mM acetic acid, 2 mM ethylenediaminetetracetic acid (EDTA), and 12.5 mM magnesium acetate; pH 8.0). TAE, magnesium acetate tetrahydrate, and filtered ultrapure water were purchased from Sigma Aldrich. For both switches, synthesis

dx.doi.org/10.1021/nl3004336 | Nano Lett. 2012, 12, 2117−2122

was performed without the control strand, which resulted in better switch performance. Thus, Switch 1 was synthesized in the OFF state, and Switch 2 was synthesized in the ON state. Once combined, the DNA solution was annealed at 90 °C for 5 min then cooled to room temperature at ~0.3 °C/min using a thermal cycler (Mastercycler, Eppendorf). The synthesized switches were purified using a 3% agarose gel at 100 V for 120 min. To identify the switch bands, the completed gels were imaged using a multiplexed fluorescence detection and gel documentation system (FluorChemQ, ProteinSimple). The excitation source was selected to excite the FAM dye, and the detection filter was chosen to pass only Cy5 emission, thus allowing clear identification of the band of well-formed FRET-based transmission lines for Switch 2, as shown in Supporting Information S2. By comparing gel bands and using Switch 2 in a control lane, Switch 1 could be located as well, even in the OFF state. Identified switch bands were excised from the gel, and the switches were extracted using Freeze 'N Squeeze columns (Bio-Rad Laboratories). Once extracted, the concentration of switches was quantified by measuring the absorption at 260 nm (BioPhotometer, Eppendorf). On the basis of the measured concentration, a stoichiometric amount of control strand was added to the scaffold solution and allowed to hybridize with the scaffold at room temperature for 30 min. With the control strand added, Switch 1 was in the ON state and Switch 2 was in the OFF state.

Dynamic optical switching of the FRET-based transmission lines was characterized using a Cary Eclipse fluorescence spectrophotometer (Agilent Technologies). The transmission lines were excited at a wavelength of 450 nm (falling within the FAM excitation spectrum but outside of the TAMRA and Cy5 excitation spectra), and fluorescence intensity at the Cy5 emission wavelength of 667 nm was monitored over time. This measurement provided a direct probe of the state of the transmission lines. Cyclic transitions between states were achieved by adding removal and return strands in increasing excess concentrations according to $m(1.5)^n$, where m is the number of moles of the switch and n is the strand injection number. Thus, the first removal strand is injected with a molar excess of 50%. To determine FRET efficiencies for the switches, the FAM dye was excited at 450 nm, and emission spectra for each device state were recorded from 500 to 800 nm.

Figures 2 and 3 summarize the results for the switching processes. In order to ensure switching of every available tile, the switching reactions shown in Figure 2 were performed with exponentially increasing concentrations of removal and return strands, as described above. Thus, each switch reaction was nonstoichiometric and involved competing reactions with the previous strands. However, to determine the control strand removal and restoration rate constants listed in Table 1, switching reactions were performed using stoichiometric amounts of all strands, and the data were fit to second-order reaction kinetics, as described in Supporting Information S3. In Figure 2, switching reaction kinetics experiments demonstrate cyclic switching of the transmission state for both switches. For Switch 1 (Figure 2a), the Cy5 fluorescence intensity decreased as the removal strand displaced the control strand and removed the TAMRA from the transmission line. When the TAMRA strand was restored, the fluorescent intensity increased to just below its original level. Conversely, for Switch 2 the Cy5 intensity increased when the control strand was displaced and the IBRQ was removed (Figure 2b). Restoring the control strand to Switch 2 caused Cy5 intensity to decrease to approximately its original level. Table 1 lists the average loss in the ON state signal (operational performance) for repeated ON-OFF-ON state transitions, calculated using the stepwise ratios of ON state Cy5 emission intensities as switching was repeated and adjusting for dilution, described in Supporting

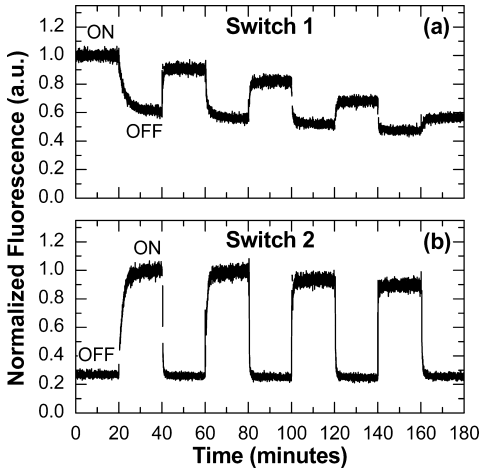

Figure 2. Switch reaction kinetics data demonstrating changes in Cy5 fluorescence intensity due to control strand removal and restoration. (a) Repeated switching of Switch 1, showing that introduction of the removal strand switches the device to its OFF state and introduction of the return strand restores it to its ON state. (b) Repeated switching of Switch 2, showing the inverse transmission behavior as Switch 1. The kinetics data were normalized by dividing by the average value of the initial ON state fluorescence. Intensity spikes produced during pipetting have been removed from the data. The raw kinetics data are provided in Supporting Information S3.

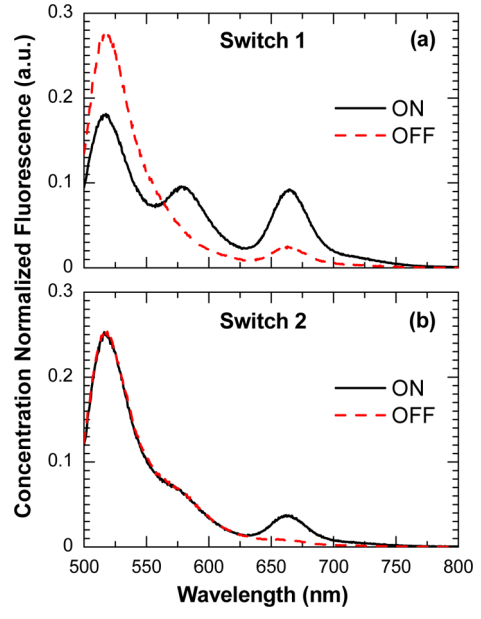

Figure 3. Full fluorescence spectra for Switch 1 (a) and Switch 2 (b) in their ON and OFF states. The emission spectra were acquired with an excitation wavelength of 450 nm to excite only the FAM dye. The peaks observed correspond to emission peaks of the individual dyes: FAM (520 nm), TAMRA (580 nm), and Cy5 (670 nm). For Switch 1, removal of the control strand eliminates the TAMRA peak and the Cy5 peak is reduced. For Switch 2, only the Cy5 peak is significantly affected by the quencher on the control strand. Each spectrum was normalized by dividing by the concentration of the switch.

dx.doi.org/10.1021/nl3004336 | *Nano Lett.* 2012, 12, 2117–2122

Table 1. Operational Data for Each Switch

	switch 1	switch 2
ON:OFF state ratio	1.6	3.7
ON state loss/gain per cycle	6% loss	2% gain
removal rate constant[a] $(M{\cdot}s)^{-1}$	$(2.69 \pm 0.05) \times 10^4$	$(1.6 \pm 0.3) \times 10^5$
restoration rate constant[a] $(M{\cdot}s)^{-1}$	$(5.2 \pm 0.4) \times 10^5$	$(3.0 \pm 0.4) \times 10^5$
FRET efficiency[b]	0.49 ± 0.09	0.19 ± 0.08

[a]Average rates from kinetics fits for two separate switches. [b]Average efficiencies for three separate switches.

Information S3. Additionally, state transition rates were calculated using equations for second-order reaction kinetics, as described below and in Supporting Information S3.

The emission spectra for each switch in both ON and OFF states are shown in Figure 3. To ensure proper stoichiometry for FRET efficiency calculations, the switches were prepared with all strands required for each state and then purified by agarose gel electrophoresis, as described above. The switch spectra demonstrate emission peaks for each dye in the transmission line and the peak intensities vary between ON and OFF states. Without TAMRA in Switch 1, the TAMRA peak vanishes and the Cy5 peak is diminished (Figure 3a). When IBRQ is absent from Switch 2, the Cy5 peak is more intense relative to Switch 2 with IBRQ (Figure 3b). Least-squares fitting of the emission spectra with individual dye spectra was used to calculate the overall FRET efficiencies for each switch, as described in ref 10 and in Supporting Information S4 and summarized in Table 1.

Dynamic control of energy transfer was clearly observed for both switch designs (Figure 2). The ratios of ON state Cy5 fluorescence to OFF state fluorescence are listed in Table 1, where it can be seen that Switch 2's ON/OFF ratio is over twice that for Switch 1. This large difference in ON/OFF ratios between switches results from differences in switch designs. For Switch 1, the OFF state was achieved by removal of the intermediate TAMRA leaving the FAM and Cy5 separated by 14 nt. Despite the small overlap of the FAM and Cy5 emission and excitation spectra, a separation of only 14 nt was insufficient to completely prevent FRET between FAM and Cy5. Evidence for FRET between FAM and Cy5 was also observed in the OFF state spectrum for Switch 1 (Figure 3a), where Cy5 emission was observed when TAMRA was absent from the tile. In contrast, very little Cy5 emission was detected in the OFF state of Switch 2 (Figure 3b). The presence of the IBRQ in the OFF state effectively quenched the Cy5 fluorescence, resulting in a much darker OFF state than that of Switch 1. The dark OFF state can be attributed to the proximity of IBQR to Cy5 (2 nt), which leads to highly efficient FRET.

In addition to displaying a low ON/OFF state ratio, Figure 2a shows that the ON state intensity for Switch 1 decreased noticeably per cycle. The average ON state intensity decrease per cycle was 6% beyond the 7% decrease expected for dilution when removal and return strands were injected. Since the OFF state intensity decrease matched the expected dilution decrease, the overall ON/OFF ratio of Switch 1 decreased per cycle. This overall intensity decrease may reflect incomplete restoration of the control strand, which could result from incomplete hybridization during two steps: (1) if the return strand did not hybridize with 100% of the removal strands, some control strands may have remained bound to removal strands; (2) if some control strands did not fully rehybridize with the scaffold strands after being released from the removal strands. To ensure complete ON and OFF state transitions, removal and return strands were injected with a 50% molar excess over the strands of the previous state. This process should ensure removal or restoration of every possible control strand, yet unintended interactions or secondary structure formation may be inhibiting control strand restoration. A similar inhibition to control strand restoration was observed for Switch 2, where the ON and OFF state intensities slightly exceeded the values expected from dilution. Although the order of the sequence domains for the control strands of Switch 1 and Switch 2 are reversed, both switches use identical toeholds. Thus, Switch 2 can be expected to display a similar lack of control strand restoration. However, since the control strand of Switch 2 contains the IBRQ, the effect was reversed compared to Switch 1, and the overall fluorescence intensity increased per cycle as an increasing fraction of Switch 2 tiles remained in the ON state. This effect is seen in the cycle gain listed in Table 1, which shows a 2% increasing dilution corrected fluorescence per cycle.

Differences in the switch designs were also reflected in the state transition rates produced by control strand removal or restoration. The removal rate for Switch 2 was almost six times greater than for Switch 1, while the restoration rates were within a factor of 2 (Table 1). The higher removal rate for Switch 2 may reflect the fact that the control strand scaffold domain for Switch 2 is four nucleotides shorter than for Switch 1. However, in both cases removal of the control strand is a three strand branch migration process that can be described as a one-dimensional random walk with a mean completion time of $n^2\tau$,[23] where n is the number of base pairs and τ is the mean step time. Estimating τ to be 50 μs or less[23] yields a maximum walk time of ~10 ms, which is significantly less than the half-time for state transitions for both switches. Thus, it is unlikely that differences in the control strand removal rates are fully accounted for by the four base pair difference for binding the control strand to the scaffold. An additional key difference in the control strands is that Switch 1's control strand is internally functionalized with TAMRA while Switch 2's control strand is functionalized with IBRQ at its 3′ end. The TAMRA functional group may interact more strongly with the switch scaffold, impeding the branch migration process and reducing the removal rate. Further studies with changes in ion species and concentration,[23] as well as modified control and scaffold domain sequences, are necessary to determine the mechanism for the differences in switch control strand removal.

In both switches, control strand removal was observed to proceed at a slower rate than control strand restoration, by roughly an order of magnitude for Switch 1 and a factor of 2 for Switch 2. These results are surprising since control strand removal involves only a single strand displacement process, whereas control strand restoration requires both strand displacement and subsequent hybridization. Additionally, as the return strands share part of their sequences with the control strands, it is possible for the return strands to interfere with the restoration of the control strands. Furthermore, the control strand of Switch 1 (Switch 2) hybridizes to the scaffold by 14 (10) bp, while the removal strand binds to the control strand with 24 (22) bp, requiring a longer branch migration process (still estimated to be less than ~30 ms).[23] In the case of Switch 1, the TAMRA functional unit can still be expected to interact with the removal strand in the same way it would with the

dx.doi.org/10.1021/nl3004336 | Nano Lett. 2012, 12, 2117−2122

scaffold. However, for Switch 2, the removal strand should not interact significantly with the IBRQ functional group. Thus, one might expect the restoration rate to be greater for Switch 2, contrary to the measured rates. Although the toeholds are different lengths (14 nt for removal and 10 nt for restoration), reaction rates are expected to remain constant for toeholds longer than about 8 nt, beyond which point the reaction rates are limited by hybridization kinetics.[24,25] For both switch reactions, the Gibbs free energy for toehold hybridization is sufficiently high that dissociation reactions can be neglected.[23] For both switches, the differences in removal and restoration rates may reflect sequence dependencies, as well as differences in the local reaction environments since the removal process occurs on the three-helix tile while the restoration process occurs on a single double-helix. Further studies beyond the scope of this report are required to elucidate the underlying mechanisms influencing the reaction rates.

The switch designs possess key differences that are evident in the emission spectra from both switches in the ON and OFF states shown in Figure 3. The primary difference between the switches is that for Switch 1, exciton transmission is controlled by the presence or absence of a mediating TAMRA dye, while for Switch 2, output dye emission is controlled by the presence or absence of a quencher. Comparison of the ON and OFF spectra of Switch 1 illustrates the manipulation of the FRET processes between the dyes. In the ON state, emission peaks are observed from all three dyes. In the OFF state, the TAMRA peak is absent, the FAM peak is increased, and the Cy5 peak is decreased, as expected. Without TAMRA, the increase in FAM emission is expected since excitonic energy transfer from FAM is less efficient to Cy5 than to TAMRA, based on both spectral overlap and relative proximities. Similarly, the decrease in Cy5 emission is expected without the mediating TAMRA. The behavior of Switch 2 is quite different from Switch 1. Since the FRET processes within the switch remain intact for both ON and OFF states, almost no change in the FAM and TAMRA emission peaks is observed between the ON and OFF spectra, and only the emission from Cy5 changes based on the presence or absence of the IBRQ.

On the basis of comparison of the ON state emission spectra from the two switches, Switch 1 displayed an overall higher transmission efficiency. The ON state transmission efficiencies were quantitatively determined using least-squares fits to the spectra obtained from linear combinations of switch tile spectra for the individual dyes, similar to the procedure described in ref 10. The fitting coefficients were used to calculate the overall efficiency of energy transfer for each switch in the ON state, as described in Supporting Information S4. The calculated ON state efficiencies are listed in Table 1 and confirm that Switch 1 exhibited higher transmission efficiency than Switch 2. The primary structural difference between the ON states of the two switches is that the transmission dyes in Switch 1 are located on a single double helix with approximately 2.38 nm between donor−acceptor pairs. In contrast, the dyes in Switch 2 are not on a single double-helix, thus the distance from the TAMRA to the input and output dye is slightly longer at approximately 3.11 nm. With the Förster radii of the FAM to TAMRA and TAMRA to Cy5 processes estimated to be 4.98 and 4.6 nm respectively,[26,27] this increase in distance should produce only a ∼14% decrease in the overall transfer efficiency. However, changes in dye orientation and nonradiative losses may be sufficient to account for the differences in transmission efficiency.

Despite the lower overall transmission efficiency of Switch 2, the ON/OFF ratio (i.e., switching efficiency) is significantly higher (Table 1). This difference results from the differences in effectively suppressing Cy5 emission in the OFF state, as seen in Figure 2. Exciton transfer to the IBRQ quencher nearly eliminates emission from Cy5 in the OFF state of Switch 2. However, in the OFF state of Switch 1, there remains significant direct energy transfer between FAM and Cy5. Despite their low spectral overlap, Cy5 emission in the OFF state of Switch 1 is nearly equal to the Cy5 emission in the ON state of Switch 2, as seen in Figure 3. Thus, although the overall transmission efficiency is lower for Switch 2, the quenching mechanism of Switch 2, dictated by a large spectral overlap between fluorophore and quencher and the proximity of the pair, does provide significantly greater control over the emission state of the transmission line.

Molecular photonic circuits show promise for information processing in nanoscale devices, and FRET is one means for directing excitonic energy flow. In this study, two methods were reported for creating switchable FRET-based excitonic transmission lines using DNA self-assembly. The switches were assembled using DNA origami techniques with a functionalized control strand that was both removable and restorable through toehold-mediated strand invasion. In the complementary switch designs, the control strand either mediates the FRET process or quenches emission from the output dye, making it possible to switch between on and off emission states. It was found that the switch design with quenched output emission exhibited a lower overall transmission efficiency but a significantly greater contrast between the on and off states. Following the work of Vyawahare et al.,[10] extension of these switch designs to longer multi-FRET transmission lines and networks should be possible. A switch design in which the FRET process is controlled by simultaneous removal or restoration of multiple intermediate dyes should yield a high efficiency transmission line with high contrast between states. Synthesis of two complementary dynamic transmission lines using DNA self-assembly indicates that it is possible to form nanoscale photonic circuits whose operation can be controlled through molecular programming. These programmable FRET-based switches could enable dynamic control over lasing in optofluidic FRET lasers[28] as well as reaction control in photochemical networks.[29] In principle, the switches reported here can be networked to implement arbitrary Boolean functions, facilitating nanoscale information processing with molecular circuitry.

■ ASSOCIATED CONTENT

Supporting Information

Strand sequences and schematic, dye information, gel purification, reaction rate calculations, switch spectra, and FRET efficiency calculations. This material is available free of charge via the Internet at http://pubs.acs.org.

■ AUTHOR INFORMATION

Corresponding Author

*E-mail: EltonGraugnard@BoiseState.edu.

Notes

The authors declare no competing financial interest.

■ ACKNOWLEDGMENTS

The authors thank Natalya Hallstrom for valuable assistance with this work. This work was supported in part by NSF IDR No. 1014922, NSF MRI No. 0923541, NIH Grant P20 RR016454, DARPA Contract No. N66001-01-C-80345, and a grant from the W. M. Keck Foundation.

■ REFERENCES

(1) Pistol, C.; Dwyer, C.; Lebeck, A. R. *IEEE Micro* **2008**, *28*, 7−19.
(2) Wagner, R. W.; Lindsey, J. S. *J. Am. Chem. Soc.* **1994**, *116*, 9759−9760.
(3) Wagner, R. W.; Lindsey, J. S.; Seth, J.; Palaniappan, V.; Bocian, D. F. *J. Am. Chem. Soc.* **1996**, *118*, 3996−3997.
(4) Förster, T. *Ann. Phys.* **1948**, *437*, 55−75.
(5) Tyagi, S.; Kramer, F. R. *Nat. Biotechnol.* **1996**, *14*, 303−308.
(6) Ohya, Y.; Yabuki, K.; Komatsu, M.; Ouchi, T. *Polym. Adv. Technol.* **2000**, *11*, 845−855.
(7) Ohya, Y.; Yabuki, K.; Hashimoto, M.; Nakajima, A.; Ouchi, T. *Bioconjugate Chem.* **2003**, *14*, 1057−1066.
(8) Ohya, Y.; Yabuki, K.; Tokuyama, M.; Ouchi, T. *Supramol. Chem.* **2003**, *15*, 45−54.
(9) Haustein, E.; Jahnz, M.; Schwille, P. *ChemPhysChem* **2003**, *4*, 745−748.
(10) Vyawahare, S.; Eyal, S.; Mathews, K. D.; Quake, S. R. *Nano Lett.* **2004**, *4*, 1035−1039.
(11) Heilemann, M.; Tinnefeld, P.; Sanchez Mosteiro, G.; Garcia Parajo, M.; Van Hulst, N. F.; Sauer, M. *J. Am. Chem. Soc.* **2004**, *126*, 6514−6515.
(12) Hannestad, J. K.; Sandin, P.; Albinsson, B. *J. Am. Chem. Soc.* **2008**, *130*, 15889−15895.
(13) Dutta, P. K.; Varghese, R.; Nangreave, J.; Lin, S.; Yan, H.; Liu, Y. *J. Am. Chem. Soc.* **2011**, *133*, 11985−11993.
(14) Stein, I. H.; Schüller, V.; Böhm, P.; Tinnefeld, P.; Liedl, T. *ChemPhysChem* **2011**, *12*, 689−695.
(15) Stein, I. H.; Steinhauer, C.; Tinnefeld, P. *J. Am. Chem. Soc.* **2011**, *133*, 4193−4195.
(16) Lilley, D. M. J.; Wilson, T. J. *Curr. Opin. Chem. Biol.* **2000**, *4*, 507−517.
(17) Steckl, A. J.; Spaeth, H.; Singh, K.; Grote, J.; Naik, R. *Appl. Phys. Lett.* **2008**, *93*, 193903.
(18) Ouellet, J.; Schorr, S.; Iqbal, A.; Wilson, Timothy, J.; Lilley, David, M. J. *Biophys. J.* **2011**, *101*, 1148−1154.
(19) Uphoff, S.; Holden, S. J.; Le Reste, L.; Periz, J.; van de Linde, S.; Heilemann, M.; Kapanidis, A. N. *Nat. Methods* **2010**, *7*, 831−836.
(20) Hannestad, J. K.; Gerrard, S. R.; Brown, T.; Albinsson, B. *Small* **2011**, *7*, 3178−3185.
(21) Yurke, B.; Turberfield, A. J.; Mills, A. P.; Simmel, F. C.; Neumann, J. L. *Nature* **2000**, *406*, 605−608.
(22) Zhang, D. Y.; Turberfield, A. J.; Yurke, B.; Winfree, E. *Science* **2007**, *318*, 1121−1125.
(23) Simmel, F. C.; Yurke, B.; Sanyala, R. J. *J. Nanosci. Nanotechnol.* **2002**, *2*, 383−390.
(24) Zhang, D. Y.; Winfree, E. *J. Am. Chem. Soc.* **2009**, *131*, 17303−17314.
(25) Yurke, B.; Mills, A. *Genet. Program. Evolvable Mach.* **2003**, *4*, 111−122.
(26) Dragan, A. I.; Klass, J.; Read, C.; Churchill, M. E. A.; Crane-Robinson, C.; Privalov, P. L. *J. Mol. Biol.* **2003**, *331*, 795−813.
(27) Massey, M.; Algar, W. R.; Krull, U. J. *Anal. Chim. Acta* **2006**, *568*, 181−189.
(28) Sun, Y.; Shopova, S. I.; Wu, C.-S.; Arnold, S.; Fan, X. *Proc. Natl. Acad. Sci. U.S.A.* **2010**, *107*, 16039−16042.
(29) Röthlingshöfer, M.; Gorska, K.; Winssinger, N. *J. Am. Chem. Soc.* **2011**, *133*, 18110−18113.